

Effect of Light Intensity on Close-Range Photographic Imaging Quality and Measurement Precision

Kaifeng Ma^{1,2}, Ximin Cui¹, Guiping Huang² and Debao Yuan¹

¹College of Geoscience and Surveying Engineering, China University of Mining and Technology, Beijing 100083, China

²School of Resources and Environment, North China University of Water Resources and Electric Power, Zhengzhou 450045, China
makf@163.com, cxm@cumtb.edu.cn

Abstract

To test the effectiveness of flash intensity in digital close-range photogrammetry, test methods for the light intensity adjustment of a ring-flash on close-range photographic imaging quality and measuring precision were researched respectively. First, according to the efficiency of the flash, the imaging characteristics, and the gray distribution of the mark points of the image, the identified method of the image gray value for subjective visual analysis was presented, and a quality standard for the close-range photographic image was provided. Then, as a precondition to obtaining the best image quality, based on the estimation theory governing measurement adjustment precision, the changes in measuring precision under conditions of different light intensity and different photographic distances were analysed, and the relationships between measurement precision and light intensity, or photographic distance, were obtained. Finally, the globally optimal imaging quality and measurement precision for any given light intensity were quantified. Experimental results indicated that the root mean square (RMS) errors of the measurement adjustment precision were 0.028 mm, 0.039 mm, and 0.085 mm; the RMS errors in the measuring precision and the corresponding coordinate repeatability were 0.038 mm, 0.053 mm, and 0.118 mm. The best imaging quality was achieved at photographic distances of 3 m, 5 m, and 7 m, with corresponding output light intensities of 1/64, 1/32, and 1/16 under certain conditions, respectively. This can satisfy the precision requirements for large-scale coordinate measurement, and provides a basis for formulating a reasonable light intensity output from a ring-flash in the digital close-range photogrammetry.

Keywords: measurement; measurement precision; light intensity; digital close-range photogrammetry; imaging quality; ring flash

1. Introduction

In recent years, with the development of the aerospace, shipbuilding, machine tool, large antenna, and heavy manufacturing industries, three-dimensional (3-d) coordinate detection methods, and their speed and accuracy, have imposed more demanding requirements on portable, fast, high-precision, non-contact, large-scale measurement technology [1-3]. Digital close-range photogrammetry research is being used to obtain digital images of the same object in two or more different locations and in different directions with the camera, by computer image feature recognition, positioning, matching, processing, and related mathematical calculations to obtain accurate 3-d coordinates of a point [4-5]. As an optical measurement system, the measurement accuracy of digital close-range photogrammetry depends on many factors: camera quality, the size and quality of reflective mark points, the algorithm used for image

feature extraction and positioning, the accuracy of image point coordinates, the intersection geometry of the camera station, the size of the object imaged, the number, and overlap, of photographs taken, *etc.* [4-11]. No analysis of their effects on the flash intensity used in a digital photogrammetry system has yet been reported. However, in visual application systems, the light source is a critical factor affecting the image quality [12]. So the effect, on the flash intensity, of digital close-range photogrammetric systems is worthy of further study.

Based on an analysis of factors affecting accuracy in digital photogrammetric systems, the effectiveness of a ring-flash light intensity adjustment test method was analyzed. Given the characteristics of the ring-macro-flash, current digital close-range photogrammetric systems, to obtain better imaging results and measurement accuracy, use them more often nowadays. In this research, using the latest model, with its higher control level (Level 12) over the light intensity output power, a ring-macro-flash (Nissin MF18) was performance-tested for use in digital close range photogrammetry. Two aspects of its influence on the image quality and measurement precision were studied, and some useful conclusions obtained. Experiments show that ring-flash use in digital close-range photogrammetry, with suitable intensity, can endow the measurement system with the best accuracy while ensuring imaging quality requirements were met. At the same time it also provided a basis for the best choice of ring-flash intensity in a digital photogrammetric system.

2. The Efficient Flash Intensity Principle

2.1. Flash Overview

A ring-macro-flash with no shadows, no vignetting flash features, is a favoured macro-photography and portrait photography tool [13]. Combined with the reflective performance and imaging needs of digital close-range photogrammetry, the ring-macro-flash is an important element of digital close-range photogrammetric systems. At present, many manufacturers try to identify its effectiveness, especially when used in digital close-range photogrammetry and, as such, its measurement accuracy is worthy of further study. The Nissin MF18 ring-macro-flash (Figure 1) was tested here. Its main parameters were: flash index (ISO 100) 16, response time 0.1 to 0.5 s, number of flashes 120 to 800, and power control level 7 (manual control) or 12 (fine control).



Figure 1. Ring-Macro-Flash Tested

2.2. The Efficient Flash Intensity Principle

In digital close-range photogrammetry, to obtain high-quality mark point images and to achieve the desired accuracy, it is necessary to use a flash to get the right amount of exposure. The effective intensity is an important parameter used to evaluate the optical characteristics of a flash-light. At the same time, because of its light not being continuous, the flash-light photometric characteristics require special instruments and test methods [14].

The effective intensity of a flash can be defined as: when under the same conditions, while observing the flash and a stable light, when adjusting the strength of the stable light source constantly, so that the flash light and stable brightness

appear consistent, the stable light emission intensity at this time is the effective intensity of the flash light source. Currently, effective intensity I_e is given by the following empirical formula [14]:

$$I_e = \frac{\int_{t_1}^{t_2} I(t) dt}{0.2 + (t_2 - t_1)} \quad (1)$$

Where, $t_2 - t_1$ is the duration of the flash light source, usually using the length of time between the two peaks in the ratio 1:4, the units being seconds; $I(t)$ is a time-varying flash light intensity.

The flash intensity can be calculated with reference to Eq. (1), and this work focuses on the influence of close-range imaging quality and measurement accuracy under certain conditions with light intensity output component size. The experiments undertaken here used a flash intensity of between 1/1 to 1/256.

3. Imaging Quality and Measurement Accuracy Estimation

3.1. Imaging Quality

In recent years, retro-reflective targets (RRT) (Figure 2 or 3(a)) have been widely used in digital close-range photogrammetry: they have unique reflective characteristics, and can be acquired with hundreds, or even thousands, of times the brightness than diffuse white flags with reflected flash light: as such they can be easily acquired by measuring the target image when "hidden", and thus the RRT image is particularly clear and prominent as a 'two value image' [4,15] (Figures 2 or 3(b)). So using a flash to improve exposure of RRT points in digital close-range photogrammetry, which makes the target more easily found and measured, also meant that the size of the flash light intensity output affected the image quality: this was because it determines the correctness of the image exposure to a certain extent. Therefore, to obtain high-quality images, we must adjust the relationship between target and background exposure to make the target clear.

At present, there are many methods of image quality evaluation [16-17], but because this measurement system used RRTs, the imaging was of the 'quasi-binary value' type: to obtain better image quality, this work used a subjective visual image gray value discrimination law to evaluate image-quality. The method was simple, fast, and practical.

The subjective visual image gray value determination method is effective for image quality evaluation using statistical analysis of a large number of images: pixel maximum grayscale values (Max_gray) can reflect the mark point image whether over exposed (Max_gray > 255, Figure 2(a)) or under-exposed (Max_gray < 170, Figure 2(b)). With neither over-, nor under-exposure, the background pixel gray scale value was between 1 and 4, which can effectively identify target points in the object orientation positions, and the image quality was optimal (Figure 2(c)); under over-exposure, although the background can be clearly identified, mark point over exposure can affect later image feature extraction, positioning, and ultimately lead to a loss of measurement accuracy. In the case of under-exposure, the general background gray value is 0, and we were unable to identify the target object orientation, thus affecting later work piece installation, adjustment, and also causing an imaging pixel gray area, or causing the number of pixels to decrease, which affects high-precision image feature extraction, positioning, and ultimately leads to decreased measuring accuracy. So over, or under-exposure reduced imaging quality.

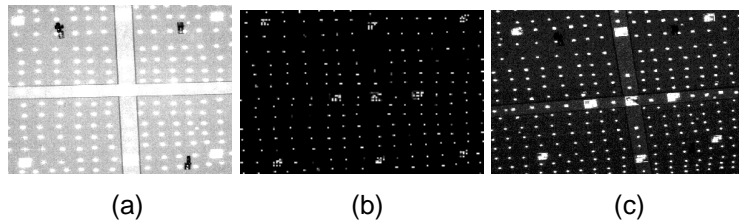


Figure 2. Detail of the Image for Capture

To facilitate a clearer understanding of mark point imaging effects and gray distributions for experiment using a Nissin MF18 flash at a distance of 3 m, the output light intensity was 1/64, and the point inside the circle in Figure 4 was used as an example (other points gave the same, or similar, results): the mark points and the gray distribution are shown in Figure 3.

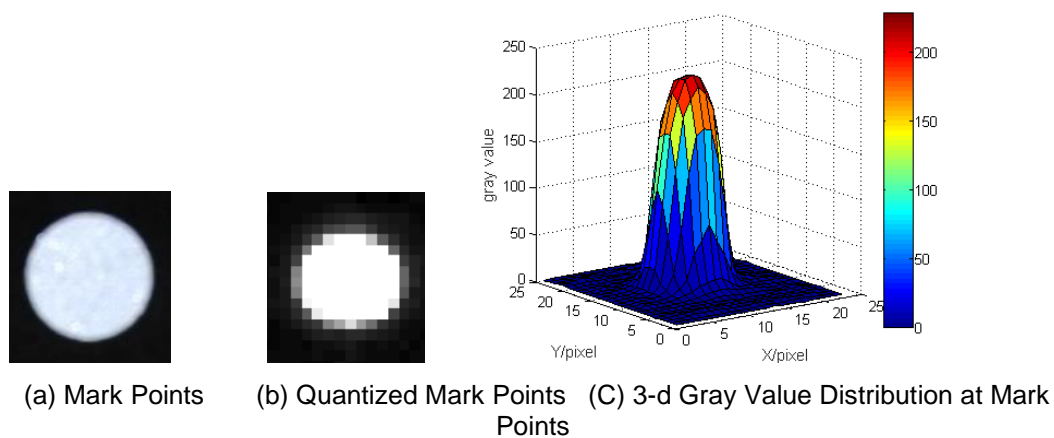


Figure 3. Image Mark Points and Gray Distribution

From Figure 3, the mark point imaging was clear, the pixel maximum gray value was 228, the pixel gray area or number of pixels was larger (23 pixels \times 25 pixels), the background pixel gray value was between 1 and 4, and the image point gray value had a normal distribution, meeting the requirements for best imaging quality.

3.2. The Theory of Measurement Accuracy Estimation

The measurement accuracy of the system was estimated: they were an important aspect of the evaluation of all of the elements thereof (including flash performance). There are a variety of evaluation accuracy indices, including: accuracy estimation, repeat measurement accuracy, *etc.* [18].

1) Accuracy estimation There are two ways to obtain an accuracy estimate: on the basis of the law of error propagation we can directly infer a functional relationship, or, after adjustment, use the statistical variance-covariance propagation theorem. This work used the latter to find the measurement accuracy of the estimated value.

Bundle adjustment and data processing in digital close-range photogrammetry entailed self-calibration bundle adjustment which calculated the unknown parameters and their corrections to find the covariance matrix (4) simultaneously, then (5) was used to calculate the unit weight error. Accuracy estimation of the measurement results of the parameters can be obtained by using (6) to (8).

Self-calibration bundle adjustment calculations are covered elsewhere [4]. The image point coordinate error equation, in matrix form, was:

$$V = AX - L \quad (2)$$

Where, v is the image point coordinates residuals, x is the unknown parameters (including the coordinates of the object points, camera station parameters, and camera parameters), L is a constant, and A is the error equation coefficient matrix obtained from the partial derivative of the image point coordinates with unknown parameters. As long as there sufficient observations, the least squares solution (2) was as follows:

$$\left. \begin{aligned} NX &= U \\ X &= N^{-1}U \\ N &= (A^T PA)^{-1}, U = A^T PL \end{aligned} \right\} \quad (3)$$

Where, the first sub-equation is a normal equation, the second sub-equation is the parametric solution, and P is the weight of each observation, the actual calculation often takes unit weights. In the normal equation, the relationship between the unknown covariance matrix and the coefficient matrix was:

$$\begin{bmatrix} Q_{11} & Q_{12} & Q_{13} \\ Q_{21} & Q_{22} & Q_{23} \\ Q_{31} & Q_{32} & Q_{33} \end{bmatrix} = N^{-1} \quad (4)$$

If the number of redundant observation were denoted by r , the mean square error of the unit weight σ_0 was:

$$\sigma_0 = \sqrt{\frac{V^T PV}{r}} \quad (5)$$

So the root mean square (RMS) error of the unknowns was:

$$m_i = \sigma_0 \sqrt{Q_{ii}} \quad (6)$$

The RMS error of the object point coordinates (X, Y, Z) only was:

$$m_1 = \sigma_0 \sqrt{Q_{11}} \quad (7)$$

Then the measurement accuracy of image point coordinate x was estimated (RMS):

$$m_x = \sqrt{\frac{\sum_{i=1}^n (V^T PV)}{n-1}} \quad (8)$$

Where, n was the total number of observations.

2) Repeatability The accuracy of inner coincidence refers to the consistency between the same measured multiple observation results under the same measurement conditions, which can reflect the repeatability, stability, and performance of parameters (in this case, the flash) of the measurement system. In digital close-range photogrammetry, test methods for the repeatability of a measuring system generally entail: under the same observation conditions, repeated measurement (m times) of the same group of object points over the same network, if the object coordinates (X_{ij}, Y_{ij}, Z_{ij}); ($i = 1, 2, \dots, m$; $j = 1, 2, \dots, n$, where m is the number of repeat measurements, n is the number of measured points), then to transform the object point coordinates of a repeated measurement into a unified coordinate system by common point coordinates, and thus obtain the RMS error of measured object coordinate difference between any two arbitrary data sets (such as K and H), that is then the repeatability, as in Eqns. (9) to (11).

$$RMS_x = \sqrt{\frac{(X_{K1} - X_{H1})^2 + (X_{K2} - X_{H2})^2 + \dots + (X_{Kn} - X_{Hn})^2}{n-1}} \quad (9)$$

$$RMS_y = \sqrt{\frac{(Y_{K1} - Y_{H1})^2 + (Y_{K2} - Y_{H2})^2 + \dots + (Y_{Kn} - Y_{Hn})^2}{n - 1}} \quad (10)$$

$$RMS_z = \sqrt{\frac{(Z_{K1} - Z_{H1})^2 + (Z_{K2} - Z_{H2})^2 + \dots + (Z_{Kn} - Z_{Hn})^2}{n - 1}} \quad (11)$$

Where, RMS_x , RMS_y , RMS_z are the RMS errors in the X, Y, Z -directions between results taken K and H times, respectively.

According to the law of combination of errors, the RMS error of a 3-d point location can be obtained from:

$$RMS_p = \sqrt{RMS_x^2 + RMS_y^2 + RMS_z^2} \quad (12)$$

Eqns. (9) to (12) give the RMS of all points between any two measurements, and we took the average as the final result (see Table 1).

4. Measurement Experiment and Results

The experiments were carried out at Zhengzhou Sunward Technologies Ltd's Laboratory (no intense light, no fluorescent lamps present). A fixed 3-d control frame (Figure 4) was used as the measurement object: it was fitted with 1250 RRT points over an area of about $3\text{ m} \times 2\text{ m} \times 0.6\text{ m}$. A digital metric camera (NIKON D3) was used, and its main parameters were: a focal length of 24 mm, a CMOS size of $36.0 \times 23.9\text{ mm}$, a resolution of 4256×2832 pixels, an iris aperture stopped to $f22.0$, and an exposure time of $1/250\text{ s}$.

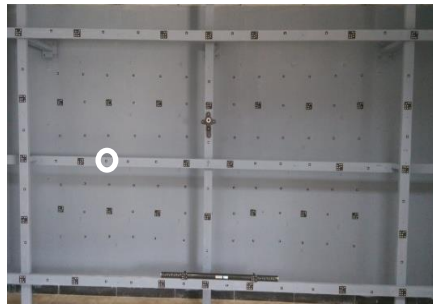


Figure 4. Layout of Mark Points

4.1. Imaging Quality Testing

To test the imaging quality, a Nissin MF18 ring-macro-flash light intensity output effect and imaging pixel grayscale was first tested. Under different output light levels, multiple images (at least three) were captured from the measured 3-d control frame as about 3 m, 5 m, 8 m, and 10 m, respectively: to take the mark points for statistical analysis of pixel gray values, the 3-d control and the object beam holder were used to form the basic level contours. In view of the imaging characteristics of the RRT itself, the maximum pixel gray value can reflect the exposure of the imaged pixel (*i.e.* whether it was over-, or under-exposed): here we adopted a Max_gray value of each mark point pixel for later statistical analysis. A point inside circle (Figure 4) was randomly selected for statistical analysis of gray values (remaining points have similar, or the same, result), and we obtained the image pixel Max_gray value under the Nissin MF18 ring-macro-flash, as shown in Figure 5.

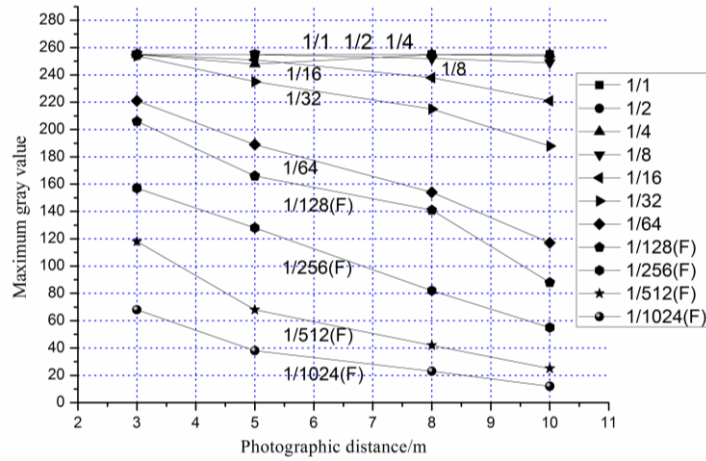


Figure 5. Maximum Gray Value of Each Mark Point Pixel

Figure 5 shows that, for a Nissin MF18 ring-macro-flash, the maximum grayscale value decreased quasi-linearly with the photographing distance given an increase in the same light output size ($< 1/8$), while it also reflected the pixel area of each mark point; when the light intensity output $\geq 1/8$, the mark point image gradually appeared overexposed, which causes the mark point pixel gray to lose the characteristics of a normal distribution: this was not conducive to subsequent data processing.

According to imaging quality standards, from Figure 5, and the experimental statistical analysis: when the flash output intensity was $1/64$, $1/32$, and $1/16$, respectively, at a distance of 3 m, 5 m, and 7 m, the measured point imaging pixel maximum gray values were 225, 235, and 240, respectively, and the background pixel gray value was between 1 and 4, thus obtaining better exposure of the subject and its background image, while achieving the best imaging quality.

4.2. Accuracy Testing Experiment

To test the effect of a Nissin MF18 ring-macro-flash on digital close-range photogrammetric accuracy, a 3-d control frame was captured at different distances (3 m, 5 m, and 7 m, respectively) at different output intensities, under the same observation conditions, using the same measuring network (*i.e.* nine positions over a uniform distribution, with repeated rotation of the camera when filming (see camera station distribution in Figure 5)). We rotated Camera, 4, with a 90° difference between the four corners and the central camera stations, with the other camera station rotating twice. Each of five groups of 28 images were post-processed using Digital Photogrammetry Software (V-STARs) to calculate the object target point 3-d coordinates (x, y, z) with bundle adjustment, respectively. Bundle adjustment accuracy estimation (BAAE) by (7) was completed to obtain the RMS values in the x, y, z -directions, maximum in each direction, and the 3-d point positions (P), respectively. The RMS values of the image point measurements (IPM) were obtained by using (8), then coordinate measurement repeatability (CMR) was computed using (9) to (12) under different light intensity conditions, respectively. Here experimental results are only given for good image quality at a certain range of light outputs ($1/256$ to $1/8$), as listed in Table 1.

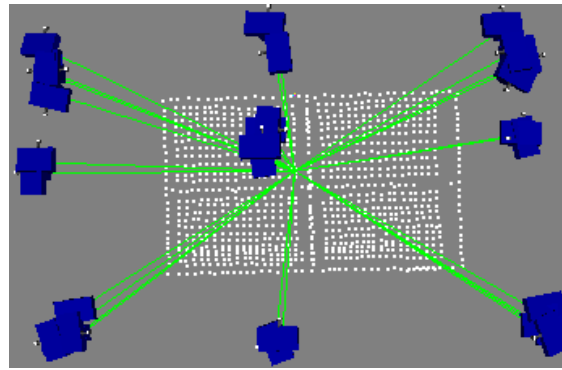


Figure 6. Distribution Diagram for each Camera Station

The actual accuracy of the measurement results showed that, the overall measurement accuracy of the results could meet the required large-scale coordinate measuring accuracy for use with a Nissin MF18 ring-macro-flash. In particular, the RMS values for bundle adjustment precision, and coordinate repetitive measurement precision were, respectively: 0.028 mm, 0.039 mm, 0.085 mm, and 0.038 mm, 0.053 mm, and 0.118 mm, in the best imaging quality seen in the triple-shadow regions (Table 1). The results showed that the measurement system had a higher measurement accuracy and good measurement repeatability under those conditions tested. Moreover, the measurement accuracy, photographing distance, and light intensity were approximately a positive, and an inverse, relationship under certain conditions.

Table 1. Statistical Data Showing Mean Values for Bundle Adjustment Precision Estimation and Coordinate Repeated Measurement Precision (Nissin MF18)

| D/ m | IO | BAAE RMS/ mm | | | | BAAE MAX/ mm | | | IPM RMS/ μm | CMR RMS/ mm | | | |
|------|----------|-----------------|-------|-------|--------------|-----------------|-------|-------|-------------------|----------------|-------|-------|--------------|
| | | X | Y | Z | P | X | Y | Z | | X | Y | Z | P |
| 3 | 1/256(F) | 0.022 | 0.010 | 0.010 | 0.026 | 0.047 | 0.024 | 0.022 | 0.310 | 0.034 | 0.013 | 0.016 | 0.039 |
| | 1/128(F) | 0.023 | 0.010 | 0.010 | 0.027 | 0.049 | 0.026 | 0.019 | 0.312 | 0.026 | 0.012 | 0.014 | 0.032 |
| | 1/64 | 0.024 | 0.010 | 0.011 | 0.028 | 0.050 | 0.026 | 0.020 | 0.310 | 0.032 | 0.016 | 0.015 | 0.038 |
| | 1/32 | 0.025 | 0.011 | 0.012 | 0.030 | 0.049 | 0.025 | 0.025 | 0.338 | 0.034 | 0.013 | 0.018 | 0.040 |
| | 1/16 | 0.027 | 0.012 | 0.013 | 0.032 | 0.048 | 0.026 | 0.029 | 0.360 | 0.035 | 0.017 | 0.021 | 0.044 |
| | 1/8 | 0.030 | 0.014 | 0.015 | 0.036 | 0.035 | 0.027 | 0.035 | 0.406 | 0.045 | 0.020 | 0.023 | 0.055 |
| 5 | 1/256(F) | 0.035 | 0.013 | 0.012 | 0.039 | 0.050 | 0.021 | 0.020 | 0.253 | 0.047 | 0.016 | 0.018 | 0.053 |
| | 1/128(F) | 0.037 | 0.013 | 0.013 | 0.042 | 0.050 | 0.022 | 0.021 | 0.276 | 0.047 | 0.017 | 0.020 | 0.054 |
| | 1/64 | 0.037 | 0.013 | 0.013 | 0.041 | 0.050 | 0.021 | 0.020 | 0.277 | 0.048 | 0.017 | 0.017 | 0.053 |
| | 1/32 | 0.035 | 0.013 | 0.012 | 0.039 | 0.049 | 0.020 | 0.020 | 0.257 | 0.048 | 0.016 | 0.017 | 0.053 |
| | 1/16 | 0.036 | 0.013 | 0.013 | 0.040 | 0.049 | 0.021 | 0.023 | 0.263 | 0.051 | 0.018 | 0.020 | 0.058 |
| | 1/8 | 0.039 | 0.014 | 0.014 | 0.044 | 0.050 | 0.022 | 0.026 | 0.287 | 0.050 | 0.020 | 0.021 | 0.058 |
| 7 | 1/256(F) | 0.072 | 0.020 | 0.018 | 0.077 | 0.097 | 0.032 | 0.032 | 0.273 | 0.098 | 0.026 | 0.026 | 0.104 |
| | 1/128(F) | 0.067 | 0.019 | 0.018 | 0.072 | 0.097 | 0.031 | 0.065 | 0.242 | 0.092 | 0.025 | 0.024 | 0.098 |
| | 1/64 | 0.069 | 0.019 | 0.017 | 0.073 | 0.092 | 0.034 | 0.028 | 0.246 | 0.113 | 0.030 | 0.027 | 0.120 |
| | 1/32 | 0.077 | 0.022 | 0.020 | 0.082 | 0.094 | 0.039 | 0.067 | 0.285 | 0.099 | 0.029 | 0.026 | 0.106 |
| | 1/16 | 0.079 | 0.023 | 0.020 | 0.085 | 0.092 | 0.035 | 0.033 | 0.294 | 0.111 | 0.030 | 0.027 | 0.118 |
| | 1/8 | 0.079 | 0.025 | 0.030 | 0.088 | 0.096 | 0.037 | 0.065 | 0.289 | 0.112 | 0.031 | 0.028 | 0.120 |

5. Conclusion

Based on influencing factor analysis of accuracy in a digital close-range photogrammetry system, ring-flash intensity adjustment test methods were presented. The performance of flash intensity in a digital close-range photogrammetry system was studied. The subjective visual image gray value discrimination methods were first proposed, and the evaluation standard of imaging quality was given. Then the imaging quality and measurement accuracy estimation theory were presented and comprehensive testing and analysis were conducted. The results showed that: the RMS values of the bundle adjustment precision were 0.028 mm, 0.039 mm, and 0.085 mm; the RMS value of the measuring precision of the coordinate repeatability was correspondingly 0.038 mm, 0.053 mm, and 0.118 mm, while the best imaging quality was achieved with photographic distances of 3 m, 5 m, and 7 m, with a corresponding output light intensity of 1/64, 1/32, and 1/16, using a NIKON D3 metric camera, respectively. It can better meet the demands of industrial, large-scale, 3-d coordinate measurement accuracy. Moreover, the measurement accuracy, photographing distance, and light intensity were in an approximately positive, inverse relationship under certain conditions.

Future research will focus mainly on experiments in an outdoor environment, and emphasize the analysis of the effect on imaging quality and measurement accuracy of direct sunlight or strong reflected light. How to take effective measures to ensure accuracy, stability, and effectiveness of the final measurement results will also be a topic for further investigation.

Acknowledgement

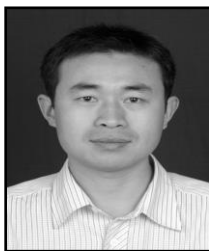
The research has been financially supported by National Natural Science Foundation of China (41071328, 41301598); National key basic research development planning (973) project (2007 CB209400). The ministry of education in the new century talents support plan funded projects (NECT-07- 07098).

References

- [1] S. Liu, Y. Dong and Z. Jiang, "Self-calibration of probe tip center for 3D vision coordinate measuring system in portable light pen", *Opt. Precision Eng.*, vol. 21, no. 7, (2013), pp. 1727-1733.
- [2] C. J., W. X. J. and W. M. Y., "3D shape modeling using a self-developed hand-held 3D laser scanner and an efficient HT-ICP point cloud registration algorithm", *Optics & Laser Technology*, vol. 45, (2013), pp. 414-423.
- [3] J. Liu, Z. Jiang and Y. Liu, "Measurement on structural deformation of load-bearing power transmission tower based on 3D optical method", *Opt. Precision Eng.*, vol. 20, no. 5, (2012), pp. 942-948.
- [4] G. Huang, "Study on the key technologies of digital close range industrial photogrammetry and applications", Tianjin: Tianjin university, (2005), pp. 67-75.
- [5] C. Long, J. Zhu and Y. Guo, "Study on close-range photogrammetry based on non-parametric measurement model", *Acta Optica Sinica*, vol. 34, no. 12, (2014), 1215004.
- [6] N. Li, "Accuracy study on close-range photogrammetry based on multi-baseline normal digital camera", Kunming: Kunming university of science and technology, (2013), pp. 63-70.
- [7] C. S. Fraser, "Optimization of networks in non-topographic photogrammetry", In: H. M. Karara, *Non-Topographic photogrammetry* (Second edition). American society for photogrammetry and remote sensing, Falls Church, Virginia, (1989), pp. 95-106.
- [8] G. Qin, "Research on underwater photogrammetry for surface measurement of satellite antenna in simulated zero-gravity conditions", Zhengzhou: The PLA information engineering university, (2011), pp. 85-100.
- [9] S. Fan, G. Huang and J. Chen, "Subpixel accuracy artificial target location using canny operator", *Journal of Zhengzhou Institute of Surveying and Mapping*, vol. 23, no. 1, (2006), pp. 76-78.
- [10] J. Zhu, J. Zou and J. Lin, "Error-compensation algorithm with high-accuracy for photographic image processing", *Acta Optica Sinica*, vol. 32, no. 9, (2012), 0912004.
- [11] L. Zhao, E. Liu and W. Zhang, "Analysis of position estimation precision by cooperative target with three feature points", *Opt. Precision Eng.*, no. 5, (2014), pp. 1190-1197.

- [12] Y. Tian and Q. Tan, "Impact of illumination on image detection accuracy", *Journal of Applied Optics*, vol. 32, no. 5, (2011), pp. 922-925.
- [13] X. Wu and X. Shi, "Macro lighting comprehensive hand Nissin ring flash MF18", *Digital Camera*, no. 9, (2012), pp. 118-119.
- [14] L. Tong, Z. Xu and W. Zhu, "Design of intensity detection system for flashing lights based on lab view", *Chinese Journal of Optics and Applied Optics*, vol. 3, no. 2, (2009), pp. 205-210.
- [15] C. S. Fraser and M. R. Shortis, "Metric exploitation of still video imagery", *Photogrammetric record*, vol. 15, no. 85, (1995), pp. 107-122.
- [16] M. Narwaria and W. Lin, "Objective image quality assessment based on support vector regression", *IEEE Transactions on Neural Networks*, vol. 21, no. 3, (2010), pp. 515-519.
- [17] X. Jin, G. Jiang and F. Chen, "Adaptive image quality assessment method based on structural similarity", *Journal of Optoelectronics Laser*, vol. 25, no. 2, (2014), pp. 378-385.
- [18] Q. Feng, "Research and practice of digital industrial photogrammetry", Zhengzhou: The PLA information engineering university, (2010), pp. 120-124.

Author



Kaifeng Ma, he received his M.Sc. in Geodesy and Survey Engineering (2007) from the Institute of Geodesy and Geophysics, Chinese Academy of Science. Now he is full teacher of North China University of Water Resources and Electric Power. Since 2012 he has been reading a doctorate in College of Geoscience and Surveying Engineering, China University of mining and Technology, Beijing. His current research interests include precision engineering and industrial measurement.